Genomic and molecular characterisation of a *Klebsiella pneumoniae* clinical isolate resistant to meropenem-vaborbactam, imipenem-relebactam, and ceftazidime-avibactam

Yu Wan[1,2,3], Joshua L. C. Wong[4], Julia Sanchez-Garrido[4], Wen Wen Low[4], Jane F. Turton[1,5], Fabio Morecchiato[6], Ilaria Baccani[6], Kirsty Dodgson[8], Gian Maria Rossolini[6,7], Neil Woodford[5], Gad Frankel[4], Elita Jauneikaite[2], Danièle Meunier[1,5], and Katie L. Hopkins[1,2,5*]

[1] AMR & HCAI Division, UK Health Security Agency, London, United Kingdom

[2] NIHR Health Protection Research Unit in Healthcare Associated Infections and Antimicrobial Resistance, Department of Infectious Disease, Imperial College London, London, United Kingdom

[3] David Price Evans Global Health and Infectious Diseases Research Group, University of Liverpool, Liverpool, United Kingdom

[4] Department of Life Sciences, Imperial College London, London, United Kingdom

[5] Public Health Microbiology Reference Microbiology Division, UK Health Security Agency, London, United Kingdom

[6] Department of Experimental and Clinical Medicine, University of Florence, Florence, Italy

[7] Careggi University Hospital, Florence, Italy

[8] Department of Medical Microbiology, Manchester University NHS Foundation Trust, Manchester, United Kingdom

Address correspondence to Katie L. Hopkins (katie.hopkins@ukhsa.gov.uk)

Abstract

This article reports an unusual *Klebsiella pneumoniae* clinical isolate, KpMVR1, resistant to meropenem-vaborbactam, imipenem-relebactam, and ceftazidime-avibactam, and investigates the underlying genetic alterations using comparative genomics and molecular experiments.

Resistance to carbapenems and third-generation cephalosporins is increasing in *K. pneumoniae* globally, restricting therapeutic options. The β-lactam/β-lactamase inhibitor combinations are widely used to circumvent β-lactamase-mediated resistance. In 2021, isolate KpMVR1 was recovered from a hospitalised patient in England. Two additional isolates with the same variable-number tandem-repeat profile—KpMVS1, collected from the same patient 42 days before KpMVR1, and KpMVS2, from another patient in the same hospital—were susceptible to meropenem-vaborbactam, imipenem-relebactam, and ceftazidime-avibactam. Illumina and nanopore whole-genome sequencing and hybrid genome assembly were conducted for these three isolates. Annotated genome assemblies were compared to identify genetic variation, and mutagenesis experiments were performed to verify predicted functional alterations.

All isolates belonged to a novel clone ST8134 and carried $bla_{\text{KPC-2}}$-like alleles (KpMVR1: $bla_{\text{KPC-157}}$; KpMVS1 and KpMVS2: $bla_{\text{KPC-2}}$) in presumptively conjugative plasmids. IS*Ec68* caused a frameshift mutation in KpMVR1's *ompK36* gene, reducing the meropenem-vaborbactam and imipenem-relebactam susceptibility. KPC-157 demonstrated decreased hydrolysis of imipenem and ceftazidime when compared with KPC-2. KpMVR1 also encoded a disrupted transcriptional repressor MarR and a destabilising mutation in AcrB, a component of the AcrAB-TolC multidrug efflux pump. In conclusion, KpMVR1 harboured complex resistance-associated genetic alterations, with evidence for *in vivo* emergence of antimicrobial resistance. Our study underlines routine screening for resistant pathogens in vulnerable patients to guide antimicrobial chemotherapy as well as the need to characterise underlying resistance mechanisms to help assess the potential for onward transmission.

Keywords

Klebsiella pneumoniae, antimicrobial resistance, combination antimicrobials, β-lactam antimicrobials, β-lactamase inhibitors, porins, medical microbiology, bioinformatics, comparative genomics, mutagenesis experiments

Data summary

Illumina and nanopore sequencing reads, hybrid genome assemblies, and anonymised metadata of isolates KpMVS1, KpMVR1, and KpMVS2 have been deposited in databases of the National Center for Biotechnology Information (www.ncbi.nlm.nih.gov) under BioProject accession PRJNA1084250, with BioSample accessions SAMN46778009 (KpMVS1), SAMN46778010 (KpMVR1), and SAMN46778011 (KpMVS2). The genome assemblies of these isolates have also been deposited in Pasteur Institute's database for *K. pneumoniae* species complex (bigsdb.pasteur.fr/klebsiella/) under ids 75608 (KpMVS1), 75609 (KpMVR1), and 75610 (KpMVS2).

Impact statement

This is the first bla_{KPC}-positive *K. pneumoniae* isolate referred to the UK's national reference laboratory with resistance to three last-resort β-lactam/β-lactamase inhibitor combinations meropenem-vaborbactam, imipenem-relebactam, and ceftazidime-avibactam, implicating *in vivo* emergence of this unusual resistance profile during prolonged antimicrobial chemotherapy. This isolate belonged to a novel clone ST8134 and harboured a plasmid-borne bla_{KPC-2}-like allele $bla_{KPC-157}$. We identified complex genetic alterations in this isolate: chromosomal large deletions, point mutations, and an IS*Ec68*-induced loss-of-function truncation of the *ompK36* porin gene. We determined the impact of KPC-2, KPC-157, and the *ompK36* truncation on the susceptibility of *K. pneumoniae* to meropenem, meropenem-vaborbactam, imipenem, imipenem-relebactam, imipenem-avibactam, aztreonam, aztreonam-avibactam, ceftazidime, ceftazidime-avibactam, and cefiderocol.

Our work underscores the need to monitor emerging resistance to beta-lactam/beta-lactamase inhibitor combinations in healthcare and to understand underlying resistance mechanisms for assessing the potential of resistance transmission.

Introduction

Meropenem and imipenem are broad-spectrum carbapenem antimicrobials parenterally administered to treat serious bacterial infections, such as those caused by Enterobacterales producing extended-spectrum β-lactamases (ESBLs) or AmpC-type cephalosporinases (AmpCs) [1–3]. Ceftazidime, a third-generation parenteral cephalosporin, is also widely used for treating severe bacterial infections, although it can be hydrolysed by ESBLs and AmpCs [4, 5]. In Gram-negative bacteria, carbapenems and cephalosporins diffuse through outer-membrane porins and enter the periplasm, where they inactivate penicillin binding proteins, disrupting cell-wall synthesis with a bactericidal effect [6–8].

Combining β-lactams with β-lactamase inhibitors in antimicrobial chemotherapy is a widely employed strategy to circumvent β-lactamase-mediated resistance in bacteria. Vaborbactam, relebactam, and avibactam are non-β-lactam inhibitors of Ambler class A β-lactamases, such as ESBLs and *Klebsiella pneumoniae* carbapenemases (KPCs), as well as class C β-lactamases (AmpCs) [9]. Moreover, avibactam inhibits several class D β-lactamases such as OXA-48 and OXA-10 [10]. These inhibitors penetrate the outer membrane (OM) of Gram-negative bacteria via porins, blocking the active sites of β-lactamases in the periplasm [9, 11].

In the UK, meropenem-vaborbactam, imipenem-relebactam, and ceftazidime-avibactam are reserved for highly selected patients [12]. Resistance to one or more of these combination antimicrobials in clinical isolates of KPC-producing *Klebsiella pneumoniae* has been previously reported [13–15]. Underlying resistance mechanisms include overproduction of KPCs or the AcrAB-TolC multidrug efflux pump, as well as gain-of-function point mutations in the bla_{KPC} gene [9, 16–18]. In addition, the disruption or transcriptional downregulation of *ompK35* (*ompF*) and *ompK36* (*ompC*), which encode non-selective porins that facilitate the diffusion of β-lactams and β-lactamase inhibitors through the OM, has also been implicated [17–20].

Here, we report and characterise a clinically significant *K. pneumoniae* isolate exhibiting resistance to ceftazidime-avibactam, meropenem-vaborbactam, and imipenem-relebactam, analysed in the

context of closely related isolates recovered in the same hospital. This was the first such isolate referred to the UK's national reference laboratory for characterisation.

Methods

Isolate collection and phenotyping

The *K. pneumoniae* isolate KpMVS1 was recovered from a lung biopsy specimen of an inpatient (hereafter, Patient 1) admitted to an intensive care unit (ICU) in England in 2021. The second *K. pneumoniae* isolate, KpMVR1, was recovered from a groin wound of the same patient 42 days later. During this ICU stay, the patient received a broad range of antimicrobials, including meropenem-vaborbactam, ciprofloxacin, and gentamicin; however, ceftazidime-avibactam and imipenem-relebactam were not used.

Species identification of the isolates and carbapenemase gene screening were performed using matrix-assisted laser desorption/ionisation-time of flight (MALDI-ToF) method and the GeneXpert system (Cepheid, USA), respectively. Initial antimicrobial susceptibility testing (AST) was conducted by the hospital, with results interpreted according to the European Committee on Antimicrobial Susceptibility Testing (EUCAST) guidelines. Both isolates were referred to the Antimicrobial Resistance and Healthcare Associated Infections (AMRHAI) Reference Unit of the UK Health Security Agency (UKHSA) for variable number tandem repeat (VNTR) typing [21] and investigation of unusual antimicrobial resistance (AMR). Furthermore, a *bla*$_{KPC}$-positive *K. pneumoniae* isolate KpMVS2 — recovered from a rectal swab of another patient (Patient 2) in the same hospital in 2020 during an outbreak investigation and sharing the same VNTR profile as KpMVS1 and KpMVR1 — was retrieved from AMRHAI's culture collection for comparison. These three isolates were subjected to whole-genome sequencing (WGS) and AST for which minimum inhibitory concentrations (MICs) of 19 antimicrobials (Table 1) and diameters of cefiderocol inhibition zones were interpreted as per EUCAST clinical breakpoints v15.0 [22].

Whole-genome sequencing

Genomic DNA of each isolate was extracted from an overnight culture using the GeneJET Kit (ThermoFisher Scientific, UK) as per the manufacturer's protocol. Short-read sequencing was conducted on a HiSeq 2500 system (Illumina, USA) by UKHSA's Colindale Sequencing Laboratory following its paired-end 101-bp protocol. Long-read sequencing was performed on MinION R9.4.1 flow cells (Oxford Nanopore Technologies [ONT], UK), with libraries prepared using the ONT Rapid Barcoding Kit SQK-RBK004.

Bioinformatics analysis

Illumina reads were trimmed and filtered with Trimmomatic v0.39 for a minimum per-read quality of Phred Q30 and minimum length of 50 bp [23]. Fast-mode basecalling and de-multiplexing of nanopore reads was conducted by guppy v4 (ONT). Nanopore reads were then trimmed and filtered for a minimum per-read quality of Q10 and minimum length of 1 kbp using fastp v0.23.4 [24]. For species confirmation and contamination assessment, taxonomical profiling of processed Illumina and nanopore reads were performed using Kraken v2.1.3, bracken v2.8, and a standard Kraken database built in September 2023 [25, 26].

Genomes of KpMVR1 and KpMVS2, with estimated nanopore read depths of 185× and 243×, respectively, were assembled using hybracter v0.5.0 (assemblers: Flye v2.9.3 and plassembler v1.5.0; sequence re-orientator: dnaapler v0.5.1; long-read polisher: medaka v1.8.0, short-read polishers: pypolca v0.2.1 and polypolish v0.5.0) [27–32]. For KpMVS1, which had nanopore reads with an estimated depth of 64×, the chromosome and plasmid sequences were assembled using Raven v1.8.3 and plassembler, respectively, and polished with nanopore and Illumina reads as for KpMVR1 and KpMVS2. Evaluation of contamination and completeness of genome assemblies were conducted with CheckM2 v1.0.2 and its database Uniref100/KO [33]. The average fold-coverage of each contig was estimated from Illumina and nanopore reads, respectively, using mosdepth v0.3.9 [34].

The genome assemblies were annotated using bakta v1.9.2 and its standard database v5.1 [35]. Multi-locus sequence typing, serotype prediction, and virulence-factor detection were performed using Kleborate v3.1.3, which incorporated Kaptive v3.1.0 [36, 37]. AMR genes were detected using AMRFinderPlus v3.12.8 with a minimum query coverage of 80% [38]. Clustered regularly interspaced short palindromic repeats (CRISPR) and CRISPR-associated (Cas) genes in chromosomes were predicted using CRISPRCasFinder [39]. For plasmids, replicon types were determined at a minimum of 80% nucleotide identity and coverage using PlasmidFinder v2.1 [40] and the mobility was predicted using mob_typer of MOB-suite v3.1.8 [41]. The fold-coverage of each KPC-encoding plasmid was divided by that of its host's chromosome to estimate the plasmid copy number. Transposons and insertion sequences (ISs) were identified using TnCentral Blast (blastn) and ISFinder, respectively [42, 43].

Chromosome and plasmids of KpMVR1 and KpMVS2 were compared against those of KpMVS1 using minimap v2.26 [44]. Identified genetic variants were annotated using snpEff v5.2 [45]. Gene Ontology terms were predicted from amino acid sequences using InterProScan v5.69-101.0 [46] with sequence alignments filtered for ≥60% query coverages. Impacts of point mutations on protein stability were predicted from wild-type protein structures in the UniProt database using Missense3D and DDMut [47–49]. The three-dimensional structure of the plasmid-encoded donor OM protein TraN was compared between KPC-encoding, IncFII-carrying plasmids pKpMVS1_1, pKpMVR1_1, and pKpMVS2_1 following the approach developed by Low *et al* (Supplementary methods) to estimate the impact of TraN alterations on the conjugation specificity and efficiency [50]. Comparison and annotations of these three plasmids were visualised using BRIG v0.95 and Proksee [51, 52]. Gene synteny was illustrated using R package gggenes [53]. Genetic alterations found in both KpMVR1 and KpMVS2 were considered unlikely to confer the unique AMR profiles of KpMVR1 and were therefore excluded from further investigation.

Functional assessment

To experimentally determine and compare the impacts of bla_{KPC-2} and $bla_{KPC-157}$ on β-lactam susceptibility in *K. pneumoniae*, KpMVS1's KPC-2-encoding plasmid pKpMVS1_1, was introduced into the plasmid-free *K. pneumoniae* laboratory strain ICC8001 (MICs: meropenem, ≤0.06 mg/L; imipenem, 0.25 mg/L; aztreonam, ≤0.125 mg/L; ceftazidime and ceftazidime-avibactam, 0.25 mg/L) through conjugation, resulting in a transconjugant $ICC8001_{KPC-2}$ [54]. Transgenic isolates $ICC8001_{KPC-157}$ and $KpMVS1_{KPC-157}$ were derived from $ICC8001_{KPC-2}$ and KpMVS1, respectively, by substituting the bla_{KPC-2} allele with $bla_{KPC-157}$. Moreover, isolates $ICC8001_{KPC-2/\Delta ompK36}$ and $ICC8001_{KPC-157/\Delta ompK36}$ were derived from $ICC8001_{KPC-2}$ and $ICC8001_{KPC-157}$, respectively, through seamless, markerless homologous recombination using mutagenesis vectors and a lambda-red based recombination system generated in previous work [54].

To predict the presence/absence of OmpK36 in the OM of KpMVR1, Sec-dependent signal peptides and their cleavage site in translated *ompK36* alleles were compared between KpMVS1 and KpMVR1 using SignalP v6.0 [55]. To validate the prediction, purification of OM proteins was performed by resuspending an overnight LB-Miller culture (VWR, USA) of each isolate in 1M HEPES (pH 7.4) and sonicating at 25% amplitude for 10 bursts of 10 seconds on, 15 seconds off each (Model 705 Sonic Dismembrator, Fisher Scientific). Isolates ICC8001 and its *ompK36*-knockout derivative, $ICC8001_{\Delta ompK36}$, were included as positive and negative controls, respectively. After separating cellular debris by centrifugation, OM proteins were obtained by centrifugation at 14,000×g for 30 mins and resuspended in 2% sarcosine/HEPES for 30 mins at room temperature. All steps were performed at 4°C on ice to preserve protein integrity unless otherwise indicated. For visualisation, 10 µg protein per isolate was separated by sodium dodecyl sulfate–polyacrylamide gel electrophoresis (SDS-PAGE) using 12% acrylamide gels and was stained with Coomassie solution (Sigma-Aldrich, USA) and imaged on a ChemiDoc XRS+ (Bio-Rad, USA).

Both progenitor isolates (KpMVS1 and KpMVR1) and the five transgenic isolates (KpMVS1$_{KPC-157}$, ICC8001$_{KPC-2}$, ICC8001$_{KPC-157}$, ICC8001$_{KPC-2/\Delta ompK36}$, and ICC8001$_{KPC-157/\Delta ompK36}$) were tested for susceptibility to meropenem, meropenem-vaborbactam, imipenem, imipenem-relebactam, imipenem-avibactam, ceftazidime, ceftazidime-avibactam, aztreonam, aztreonam-avibactam, and cefiderocol (in iron-depleted medium) by the reference broth microdilution method as per the EUCAST guidance [56, 57]. Any MIC change above a two-fold difference between two isolates was considered notable.

Results

Phenotypes of isolates

Isolates KpMVS1 and KpMVR1, obtained 42 days apart from Patient 1 with recurrent *K. pneumoniae* infections, and KpMVS2, obtained from Patient 2 in the same hospital, were identified as *K. pneumoniae* by both MALDI-ToF and WGS. In the ICU where KpMVS1 and KpMVR1 were recovered, all patients were screened for carriage of carbapenemase-producing Enterobacterales (CPE) on admission using PCR, and the resistance profile of KpMVR1 was unique among all identified CPE isolates from the ICU during Patient 1's stay.

Based on AST results from the AMRHAI Reference Unit (Table 1), KpMVR1 was resistant to meropenem-vaborbactam (MIC>256 mg/L), ceftazidime-avibactam (MIC=16 mg/L), and ciprofloxacin (MIC>4 mg/L), whereas KpMVS1 and KpMVS2 were susceptible to these antimicrobial agents (MICs: meropenem-vaborbactam ≤0.064 mg/L; ceftazidime-avibactam 1 mg/L; ciprofloxacin ≤0.125 mg/L). Notably, KpMVS2 was resistant to cefiderocol. Further AST discovered that the imipenem-relebactam MIC of KpMVR1 (512 mg/L, resistant) was 2048 times that of KpMVS1 (0.25 mg/L, susceptible) (Table 2). Moreover, KpMVR1 exhibited a >4-fold increase in the temocillin MIC (>128 mg/L) and a >8-fold reduction in the cefepime MIC (4 mg/L, susceptible, increased exposure) compared with KpMVS1 (temocillin: 32 mg/L; cefepime: >32 mg/L, resistant).

Table 1. Antimicrobial minimum inhibitory concentrations (MICs; mg/L) determined by UKHSA's AMRHAI Reference Unit and susceptibility interpretations (as per EUCAST clinical breakpoints v15.0) of three *K. pneumoniae* clinical isolates. Abbreviations: MEM, meropenem; VAB, vaborbactam; IPM, imipenem; ETP, ertapenem; CET, ceftolozane; TZB, tazobactam; CFD, cefiderocol; FEP, cefepime; CAZ, ceftazidime; AVI, avibactam; CTX, cefotaxime; FOX, cefoxitin; TMC, temocillin; AMP, ampicillin; AMX, amoxicillin; CAV, clavulanate; PIP, piperacillin; ATM, aztreonam; AMK, amikacin; GEN, gentamicin; CST, colistin; CIP, ciprofloxacin; MB, monobactam. Susceptibility interpretations: R, resistant; I, susceptible, increased exposure; S, susceptible.

	Carbapenem				**Cephalosporin**							**Penicillin**				**MB**	**Aminoglycoside**		**Others**	
Isolate	**MEM-VAB**	**MEM**	**IPM**	**ETP**	**CET-TZB**	**CFD***	**FEP**	**CAZ**	**CAZ-AVI**	**CTX**	**FOX‡**	**TMC‡**	**AMP**	**AMX-CAV**	**PIP-TZB**	**ATM**	**AMK‡**	**GEN‡**	**CST‡**	**CIP**
KpMVR1	>256 (R)	>16 (R)	>128 (R)	>4 (R)	16 (R)	(S)	4 (I)	256 (R)	16 (R)	8 (R)	>64	>128	>32 (R)	>32 (R)	>64 (R)	16 (R)	2	0.5	≤0.5	>4 (R)
KpMVS1	0.064 (S)	>16 (R)	64 (R)	>4 (R)	>16 (R)	(S)	>32 (R)	128 (R)	1 (S)	64 (R)	>64	32	>32 (R)	>32 (R)	>64 (R)	>32 (R)	≤1	≤0.25	≤0.5	≤0.125 (S)
KpMVS2	0.032 (S)	16 (R)	16 (R)	>4 (R)	>16 (R)	(R)	>32 (R)	64 (R)	1 (S)	16 (R)	32	8	>32 (R)	>32 (R)	>64 (R)	>32 (R)	≤1	≤0.25	1	≤0.125 (S)

* CFD susceptibility was determined using disc diffusion. ‡ Interpretations were not available according to EUCAST guidelines.

Table 2. Minimum inhibitory concentrations of beta-lactam antimicrobials and susceptibility interpretations (as per EUCAST clinical breakpoints v15.0, where applicable) of progenitor and transgenic *K. pneumoniae* isolates determined in the experiments for functional assessment. Subscripts in isolate names indicate transgenic isolates and corresponding genotypes. Abbreviations: MEM, meropenem; VAB, vaborbactam; IPM, imipenem; REL, relebactam; ATM, aztreonam; AVI, avibactam; CAZ, ceftazidime; CFD, cefiderocol, tested in iron-depleted Mueller Hinton broth; NT, not tested. Interpretations of antimicrobial susceptibility: R, resistant; I, susceptible upon increased antimicrobial exposure; S, susceptible. Notations: *ompK36*fs, frameshifted *ompK36*; Δ*ompK36*, deletion of *ompK36*.

Isolate	**Genotype**		**Minimum Inhibitory Concentration (mg/L) and interpretation**									
			MEM	**MEM-VAB**	**IPM**	**IPM-REL**	**IPM-AVI**	**ATM**	**ATM-AVI**	**CAZ**	**CAZ-AVI**	**CFD**
KpMVR1	*bla*$_{KPC-157}$	*ompK36*fs	512 (R)	256 (R)	512 (R)	512 (R)	NT	16 (R)	4 (S)	8 (R)	8 (S)	0.5 (S)
KpMVS1	*bla*$_{KPC-2}$	*ompK36*	32 (R)	≤0.06 (S)	32 (R)	0.25 (S)	≤0.5	512 (R)	0.25 (S)	32 (R)	0.5 (S)	0.25 (S)
KpMVS1$_{KPC-157}$	*bla*$_{KPC-157}$	*ompK36*	16 (R)	≤0.06 (S)	8 (R)	8 (R)	≤0.5	2 (I)	0.25 (S)	1 (S)	0.25 (S)	≤0.06 (S)
ICC8001$_{KPC-2}$	*bla*$_{KPC-2}$	*ompK36*	16 (R)	≤0.06 (S)	16 (R)	0.25 (S)	≤0.5	512 (R)	0.125 (S)	32 (R)	0.25 (S)	0.25 (S)
ICC8001$_{KPC-157}$	*bla*$_{KPC-157}$	*ompK36*	16 (R)	≤0.06 (S)	4 (I)	4 (R)	≤0.5	1 (S)	0.125 (S)	0.5 (S)	0.125 (S)	≤0.06 (S)
ICC8001$_{KPC-2/\Delta ompK36}$	*bla*$_{KPC-2}$	Δ*ompK36*	256 (R)	2 (S)	256 (R)	2 (S)	NT	>1024 (R)	0.25 (S)	16 (R)	0.5 (S)	0.25 (S)
ICC8001$_{KPC-157/\Delta ompK36}$	*bla*$_{KPC-157}$	Δ*ompK36*	256 (R)	4 (S)	256 (R)	128 (R)	NT	4 (I)	0.25 (S)	1 (S)	0.5 (S)	0.25 (S)

Table 3. Genetic characteristics of the three *K. pneumoniae* clinical isolates. Abbreviation: AMR, antimicrobial resistance. Each hit of plasmid replicons covered the full length of its reference sequence in the PlasmidFinder database.

Isolate	Sequence	Category	Length (bp)	Plasmid type	Nucleotide identity to template	Plasmid mobility	AMR gene
KpMVS1	KpMVS1	Chromosome	5,404,514				bla_{SHV-36}, *fosA10*
	pKpMVS1_1	Plasmid	111,397	IncFII/repB(R1701)	IncFII(pKP91): 100%; repB(R1701): 99.52%	Conjugative	bla_{KPC-2}
	pKpMVS1_2	Plasmid	41,868	IncFII(pMET)	IncFII(pMET): 98.09%	Non-mobilisable	
	pKpMVS1_3	Plasmid	4,809	Col(pHAD28)	Col(pHAD28): 92.37%	Non-mobilisable	
	pKpMVS1_4	Plasmid	4,439	Col(pHAD28)/Col440II	Col(pHAD28): 93.13%; Col440II: 97.52%	Mobilisable	
	pKpMVS1_5	Plasmid	3,258	Unknown	Not detected	Non-mobilisable	
	pKpMVS1_6	Plasmid	1,917	Col(pHAD28)	Col(pHAD28): 100%	Mobilisable	
KpMVR1	KpMVR1	Chromosome	5,292,801				bla_{SHV-36}, *fosA10*
	pKpMVR1_1	Plasmid	111,174	IncFII/repB(R1701)	IncFII(pKP91): 100%, repB(R1701): 99.52%	Conjugative	$bla_{KPC-157}$
	pKpMVR1_2	Plasmid	41,868	IncFII(pMET)	IncFII(pMET): 98.09%	Non-mobilisable	
	pKpMVR1_3	Plasmid	4,809	Col(pHAD28)	Col(pHAD28): 92.37%	Non-mobilisable	
	pKpMVR1_4	Plasmid	4,439	Col(pHAD28)/Col440II	Col(pHAD28): 93.13%; Col440II: 97.52%	Mobilisable	
	pKpMVR1_5	Plasmid	3,258	Unknown	Not detected	Non-mobilisable	
	pKpMVR1_6	Plasmid	1,917	Col(pHAD28)	Col (pHAD28): 100%	Mobilisable	
KpMVS2	KpMVS2	Chromosome	5,354,507				bla_{SHV-36}, *fosA10*
	pKpMVS2_1	Plasmid	116,795	IncFII/IncR	IncFII(pKP91): 100%; IncR: 99.6%	Conjugative	bla_{KPC-2}
	pKpMVS2_2	Plasmid	41,868	IncFII(pMET)	IncFII(pMET): 98.09%	Non-mobilisable	
	pKpMVS2_3	Plasmid	4,808	Col(pHAD28)	Col (pHAD28): 92.37%*	Non-mobilisable	
	pKpMVS2_4	Plasmid	4,187	Col(pHAD28)	Col (pHAD28): 92.37%*	Non-mobilisable	
	pKpMVS2_5	Plasmid	3,258	Unknown	Not detected	Non-mobilisable	
	pKpMVS2_6	Plasmid	1,917	Col(pHAD28)	Col (pHAD28): 100%	Mobilisable	
	pKpMVS2_7	Plasmid	240,297	IncFII(pKP91)/IncFIB(K)	IncFII(pKP91): 84.98%; IncFIB(K): 98.93%	Conjugative	

* Two hits of the Col(pHAD28) template sequence in the PlasmidFinder database differed between pKpMVS2_3 and pKpMVS2_4 by seven nucleotide substitutions (95% nucleotide identity) despite their same percent identity to the template.

Table 4. Chromosomal genetic variation in isolate KpMVR1 identified via comparison against its progenitor KpMVS1. Coordinates refer to locations in the reference sequence of the KpMVS1 chromosome. Variants shared by both KpMVR1 and KpMVS2 against their common reference sequence of KpMVS1 are indicated by asterisks following the coordinates. The "^" sign indicates an insertion between two consecutive bases in the reference sequence. Abbreviations: CRISPR, clustered regularly interspaced short palindromic repeats; Cas: CRISPR-associated genes; Del, deletion; Ins, insertion; fs, frameshift.

Location	Locus	Product	Variant type	DNA change	Protein change
455179	*rrl*	23S rRNA	Substitution	G>T	
1050491 – 1070213	Multiple	Type I-E CRISPR-Cas system, *etc*. (Figure S3, Table S3)	Deletion	Deletion of 19,723 bp	Loss of production
1113441 – 1113446	*flhA*	Formate hydrogenlyase transcriptional activator	Deletion	Deletion of 6 bp	L367Del, T368Del
1218110^1218111 *	*rrl*	23S rRNA	Insertion	Insertion of base G	
1578603	*gyrA*	DNA topoisomerase (ATP-hydrolyzing) subunit A	Substitution	248C>A	S83Y
1588108^1588109	*ompK36*	Outer membrane porin OmpK36	Insertion	Insertion of IS*Ec68*	Amino acid substitutions
1724677^1724678 *	*xylB*	Xylulose kinase	Insertion	Insertion of base G	I236fs
1792900	*rfbD*	UDP-galactopyranose mutase	Substitution	578T>A	M193K
1819375^1819376	Intergenic		Insertion	Insertion of base C	
2183835^2183836 *	Intergenic		Insertion	Insertion of base T	
2183837 *	Intergenic		Substitution	A>T	
2201799–2256547	Multiple	Multiple products including transporters (Figure 1, Table S2)	Deletion	Deletion of 54,749 bp	Loss of production
2759671–2759685	*marR*	Multiple-AMR (Mar) transcriptional repressor MarR	Deletion	Deletion of bases 263–277	P88–D92Del, K93Q
3157221^3157222 *	Intergenic		Insertion	Insertion of base C	
3189754 – 3223285 *	Multiple	Multiple products (Figure S4, Table S4)	Deletion	Deletion of 33,532 bp	Loss of production
3274833	*phoQ*	Two-component system sensor histidine kinase	Substitution	C>T	T156I
3580334 – 3585227 *	Multiple	IS*3H* composite transposon (Figure S5, Table S5)	Deletion	Deletion of 4,894 bp	Loss of production
4104884	*acrB*	Multidrug efflux RND transporter permease subunit AcrB	Substitution	T>G	L667R
4262704^ 4262705	*ecpR*	Regulator protein EcpR	Insertion	Insertion (2 bp)	I115fs
4723928	*rrl*	23S ribosomal RNA	Deletion	Deletion of base C	
5349457	*rrl*	23S ribosomal RNA	Deletion	Deletion of base C	

Genetic characteristics of isolates

All three isolates belonged to *K. pneumoniae* clone ST8134, a novel single-locus variant of ST240, and were predicted to share the O1αβ,2β O-antigen type and K62 capsular polysaccharide type. Sequence lengths, plasmid replicons, and AMR genes determined in hybrid genome assemblies are summarised in Table 3. KpMVR1 and KpMVS1 shared the same plasmid types IncFII/repB(R1701), IncFII(pMET), Col(pHAD28), and Col(pHAD28)/Col440II, whereas KpMVS2 possessed unique plasmid types IncFII/IncR and IncFII(pKP91)/FIB(K).

KpMVS1 carried $bla_{\text{KPC-2}}$ on the 111.4 kbp IncFII(pKP91)/repB(R1701) plasmid pKpMVS1_1. A plasmid of the same type was identified in KpMVR1 (pKpMVR1_1, 111.2 kbp) and carried $bla_{\text{KPC-157}}$, which differed from $bla_{\text{KPC-2}}$ by a single missense mutation (392A>G) resulting in an N131S amino acid substitution within the enzyme's active site [58], where N131 bounds to relebactam, avibactam, and vaborbactam through a hydrogen bond [59–61]. Notably, pKpMVR1_1 differed from pKpMVS1_1 by 285 nucleotide substitutions, 14 deletions, and three insertions. These variants were concentrated in two genomic regions involved in plasmid transfer and maintenance (Figure S1), suggesting recombination between plasmids. Another plasmid type, IncFII(pKP91)/IncR, in KpMVS2 harboured $bla_{\text{KPC-2}}$. All these KPC-encoding plasmids were predicted to be conjugative (relaxase type: MOBF; mating pair formation type: MPF_F), and each carried a variant of the Tn*4401a* transposon harbouring $bla_{\text{KPC-2}}$ or $bla_{\text{KPC-157}}$, with 1–2 SNPs between each pair of transposons (Table S1, Figure S1). The comparison between fold-coverages of contigs suggested that each of these three isolates carried a single copy of the KPC-encoding plasmid. Other AMR genes detected in these isolates were chromosomal β-lactamase gene bla_{SHV} (variant $bla_{\text{SHV-36}}$) and fosfomycin resistance gene *fosA10*, which are both intrinsic to *K. pneumoniae* [62–64].

The chromosome of KpMVR1 differed from that of KpMVS1 by six single-nucleotide polymorphisms (SNPs), seven insertions, and eight deletions (including four large deletions illustrated in Figures 1 and S2–5). Seven of these genetic variants were also identified in KpMVS2 (Table 4),

which differed from KpMVS1 by 129 SNPs, 13 insertions, and seven deletions. Two large deletions (19.7 kbp and 4.9 kbp) in KpMVR1 could be attributed to an IS-mediated deletion that had previously been observed in *Escherichia coli* (Figures S3 and S5) [65]. Notably, KpMVR1 exhibited deletion of a 54.7-kbp region that comprised operons producing an AcrAB-like multidrug efflux pump and an additional ABC-type Fe^{3+}-siderophore transport system in both KpMVS1 and KpMVS2 (Figure 1 and Table S2). Each of the three isolates carried a single copy of the *acrRAB* operon and *tolC* gene, which combine to produce the AcrAB-TolC multidrug efflux pump. However, the permease AcrB in KpMVR1 differed from that in KpMVS1 and KpMVS2 by a destabilising mutation L667R outside the protein's transmembrane domains.

As for the biosynthesis of siderophores and transport of the iron-siderophore complex, which facilitate cefiderocol to penetrate the OM [66], KpMVS1, KpMVR1, and KpMVS2 were predicted to possess complete enterobactin production and iron-enterobactin transport systems, while none of the yersiniabactin, colibactin, aerobactin, or salmochelin loci were detected, corresponding to a Kleborate virulence score of zero. All three isolates shared the same 19-kbp chromosomal region harbouring a cluster of enterobactin-synthesising genes *entA–F and entH*, enterobactin-exporter gene *entS*, and iron-enterobactin transporter genes *fepA–D* and *fepG*.

Compared with the ciprofloxacin-susceptible isolates KpMVS1 and KpMVS2, KpMVR1 harboured a nucleotide substitution 248C>A in the DNA gyrase gene *gyrA*, resulting in the GyrA mutation S83Y, which is known to reduce ciprofloxacin susceptibility [67]. The three isolates also carried a single copy of the *marRAB* operon. However, KpMVR1 exhibited a unique 15-bp in-frame deletion in the non-essential transcriptional repressor gene *marR* within the *marRAB* operon, causing a loss of five amino acids and an amino acid substitution within the DNA-binding region of MarR (Table 4) [68].

Seven bases at the 5' end of *ompK36* in KpMVR1 were truncated by an additional copy of insertion sequence IS*Ec68* (three copies in KpMVS1 and KpMVS2, respectively), resulting in a frameshift

mutation that replaced the first three amino acids at the N-terminal of OmpK36 with 12 amino acids (Figure 2). The native 21 N-terminal amino acids of OmpK36 encode a Sec-dependent signal sequence (UniProtKB accession: A0A0H3H0Y2) that is required for translocating this protein to the inner membrane of *K. pneumoniae* (Figure 2B) [69]. The signal sequence is subsequently cleaved and OmpK36 is then folded and inserted into the OM (where the protein is functionally active as a porin) in a Bam-complex dependent fashion, a process facilitated by a C-terminal recognition sequence [70]. Whilst *ompK36* from KpMVS1 and KpMVS2 is predicted to encode a complete sec-dependent signal sequence, the 12 amino acids insertion combined with the deletion of three amino acids in OmpK36 from KpMVR1 is predicted to hinder this protein's translocation to the OM according to the disrupted signal sequence (Figure S6). These predictions were confirmed by polyacrylamide gel electrophoresis of OM preparations, followed by Coomassie staining, that a band corresponding to OmpK36 was present in KpMVS1 but absent in KpMVR1 (Figure 2C). Therefore, the disruption of the Sec-dependent signal sequence of OmpK36 is functionally equivalent to deletion of *ompK36*.

Regarding the plasmid-encoded TraN proteins, $TraN_{pKpMVR1\_1}$ and $TraN_{pKpMVS2\_1}$ were identical (NCBI protein accession: WP_049192820.1) and differed from $TraN_{pKpMVS1\_1}$ (WP_436914186.1) by six amino acid substitutions (Table S6). Phylogenetic analysis revealed that these proteins belonged to the specialist TraNβ group (Figure S7), which has a narrow host range [50, 71]. Pairwise structural comparison between $TraN_{pKpMVR1\_1}$ ($TraN_{pKpMVS2\_1}$), $TraN_{pKpMVS1\_1}$, and the prototype TraNβ protein $TraN_{pKpQIL}$ showed high consistency (Figures S8), and no amino acid substitution occurred in the characteristic distal β-hairpin (Figure S9), suggesting that the variation in TraN sequences across plasmids pKpMVR1_1, pKpMVS1_1, pKpMVS2_1, and pKpQIL is unlikely to affect the conjugation specificity [72].

Impact of genetic alterations on antimicrobial resistance

The substitution of bla_{KPC-2} with $bla_{KPC-157}$ in KpMVS1 ($KpMVS1_{KPC-157}$) and the transconjugant $ICC8001_{KPC-2}$ ($ICC8001_{KPC-157}$) did not affect the susceptibility to meropenem, meropenem-

vaborbactam, or imipenem-avibactam but led to a fourfold reduction in the imipenem MIC and a 16- to 32-fold increase in imipenem-relebactam MIC (Table 2). Moreover, this allelic substitution resulted in a 256- to 512-fold reduction in the aztreonam MIC, a 32- to 64-fold reduction in the ceftazidime MIC, and a ≥4-fold reduction in the cefiderocol MIC, but had no effect on the MICs of aztreonam-avibactam or ceftazidime-avibactam. Notably, imipenem and imipenem-relebactam MICs of each KPC-157-producing isolate were identical (Table 2). These findings suggest that KPC-157 has a weaker capacity to hydrolyse imipenem, aztreonam, ceftazidime, and cefiderocol than KPC-2, and that—unlike vaborbactam and avibactam, which inhibit both KPC variants—relebactam inhibits KPC-2 but not KPC-157, which is consistent with a previous report [59].

Knocking out *ompK36* from the ICC8001 chromosome ($ICC8001_{KPC\text{-}2/\Delta ompK36}$ and $ICC8001_{KPC\text{-}157/\Delta ompK36}$) led to a 16-fold increase in the MICs of both meropenem and imipenem, a >33-fold increase in the meropenem-vaborbactam MIC, an 8- to 32-fold increase in the imipenem-relebactam MIC, and a more than twofold increase in the aztreonam MIC (Table 2). These findings are consistent with the role of OmpK36 as an entry route for β-lactams and β-lactamase inhibitors to penetrate the OM [73]. Nevertheless, when comparing MICs of ceftazidime, ceftazidime-avibactam, and cefiderocol before and after knocking out *ompK36* from $ICC8001_{KPC\text{-}2}$ and $ICC8001_{KPC\text{-}157}$, only two pairs of MICs exhibited notable increases (from 0.125 mg/L to 0.5 mg/L for ceftazidime-avibactam, and from ≤0.06 mg/L to 0.25 mg/L for cefiderocol), while the others showed no appreciable changes, suggesting alternative routes of avibactam's entry. More generally, the comparison between β-lactam MICs with and without β-lactamase inhibitors for isolates KpMVR1, $ICC8001_{KPC\text{-}2/\Delta ompK36}$, and $ICC8001_{KPC\text{-}157/\Delta ompK36}$ in Table 2 indicates that these inhibitors penetrated the OM via routes other than OmpK36, effectively inhibiting β-lactamases.

The chromosomes of KpMVR1, KpMVS1, and ICC8001 derivatives harboured the same cluster of *ent* and *fep* genes within a 19-kbp region encoding an ABC-type Fe^{3+}-siderophore transporter associated with the cefiderocol susceptibility [66]. These isolates did not exhibit any notable difference

in cefiderocol MICs despite KpMVR1's loss of the 54.7-kbp chromosomal region harbouring *fep*-like genes (Table S2), suggesting alternative entry routes of cefiderocol.

Discussion

In the UK, meropenem-vaborbactam and imipenem-relebactam are recommended for treating adult patients (≥18 years of age) with severe multidrug-resistant infections where therapeutic options are limited, and ceftazidime-avibactam is recommended as an alternative when the disease-causing bacterium produces class D carbapenemase (*e.g.*, OXA-48) [74–76]. Prevalence of resistance in Enterobacterales to any of these three combination antimicrobials was 1–5% across the globe as of 2022 despite regional variation [17, 77–81]. Therefore, the discovery of *K. pneumoniae* isolate KpMVR1, which exhibited unusual resistance to meropenem-vaborbactam, imipenem-relebactam, and ceftazidime-avibactam, in a seriously ill patient is particularly worrisome. The small number of chromosomal SNPs (n=6) and indels (n=10; ≤15 bp each) identified in KpMVR1 when compared with KpMVS1, Patient 1's exposure to meropenem, meropenem-vaborbactam, and fluoroquinolones, and the unique antibiogram of KpMVR1 in the ICU altogether support the suspected *in vivo* emergence of meropenem-vaborbactam, ceftazidime-avibactam, imipenem-relebactam, and ciprofloxacin resistance in the same *K. pneumoniae* strain during this patient's hospital stay. A similar shift in the ceftazidime-avibactam susceptibility profile of *K. pneumoniae* has been reported during treatment using meropenem followed by ceftazidime-avibactam [82].

KPC-2 is known to confer carbapenem resistance in Gram-negative bacteria but can be effectively inhibited by vaborbactam, avibactam, and relebactam [83]. Here, we have experimentally determined the effect of carbapenemase KPC-157 on the susceptibility to carbapenems and cephalosporins with or without β-lactamase inhibitors. Our results indicate that KPC-157 does not differ from KPC-2 in its interaction with meropenem or meropenem-vaborbactam. Therefore, the presence of $bla_{\text{KPC-157}}$ in the single-copy plasmid pKpMVR1_1 alone cannot explain the high-level meropenem-vaborbactam

363 resistance observed in KpMVR1. Notably, KPC-157 appears less capable of hydrolysing imipenem,
364 aztreonam, ceftazidime, and cefiderocol than KPC-2, and is inhibited by vaborbactam and avibactam
365 but not by relebactam.

366 Isolate KpMVR1 showed genetic changes that may alter the antimicrobial permeability of its OM
367 when compared with isolate KpMVS1. Resulting from an IS-induced sequence disruption, the
368 hindered translocation of OmpK36 to the OM is predicted to hamper the influx of β-lactams and β-
369 lactamase inhibitors into the periplasm, hence elevated MICs of carbapenems and cephalosporins
370 tested in Table 2 with and without β-lactamase inhibitors. Such hampered antimicrobial and inhibitor
371 influx might be further compromised by a decreased expression of *ompK35* in KpMVR1 as a result of
372 the in-frame, presumptively inactivating deletion within the repressor gene *marR* and the consequent
373 upregulation of the *marA* gene [84]. Moreover, the inactivation of *marR* is known to increase the
374 production of the AcrAB-TolC efflux pump, conferring low-level cross-resistance to antimicrobials
375 including β-lactams and ciprofloxacin [85]. However, this upregulation of AcrAB-TolC in KpMVR1
376 might not alter its antimicrobial susceptibility owing to the possibly destabilised AcrB. Therefore, the
377 high-level ciprofloxacin resistance in KpMVR1 could be primarily driven by the combination of the
378 *gyrA* mutation S83Y and the absence of OmpK36 in this isolate's OM [67, 86].

379 This study is limited to three *K. pneumoniae* isolates belonging to the same clone, with only one
380 isolate (KpMVR1) exhibiting elevated MICs of meropenem-vaborbactam, imipenem-relebactam,
381 aztreonam-avibactam, and ceftazidime-avibactam. KpMVR1 harboured multiple AMR-associated
382 genetic alterations. Broader surveillance of genetic variants similar to those identified in KpMVR1 is
383 needed to assess the prevalence and clinical relevance of these putative resistance mechanisms.
384 Although we experimentally validated the individual contributions of $bla_{\text{KPC-157}}$ and Δ*ompK36* to
385 antimicrobial susceptibility, the genetically reconstructed isolates could not fully replicate the same
386 level of MIC increments as KpMVR1, suggesting that other genetic or regulatory mechanisms may be
387 involved, which remain to be elucidated. Transcriptomic and proteomic profiling could be performed

in the future to determine whether regulatory mechanisms also contribute to the observed AMR in KpMVR1.

At the nation level, a review of routine surveillance and reference laboratory samples from 2016-2020 revealed only low levels of resistance to ceftazidime-avibactam in the UK [81]. However, it remains essential that emerging resistance to ceftazidime-avibactam and novel β-lactam/β-lactamase inhibitor combinations is promptly identified and reported through UKHSA's Second Generation Surveillance System and referral of such isolates to the AMRHAI Reference Unit. Additionally, our study highlights the importance of monitoring the evolving antimicrobial susceptibility profiles of bacterial pathogens within patients during antimicrobial therapy.

Funding information

This work was mainly funded by the UKHSA. YW is a research fellow funded by the David Price Evans Endowment (grant number: UGG10057) at the University of Liverpool and was an Imperial Institutional Strategic Support Fund Springboard Research Fellow, funded by the Wellcome Trust and Imperial College London (grant number: PSN109). YW, EJ, DM, and KLH are affiliated with the National Institute for Health and Care Research Health Protection Research Unit in Healthcare Associated Infections and Antimicrobial Resistance at Imperial College London in partnership with the UKHSA, in collaboration with, Imperial Healthcare Partners, University of Cambridge and University of Warwick (grant number: NIHR200876). The views expressed in this article are those of the authors and not necessarily those of the NHS, the National Institute for Health Research, or the Department of Health and Social Care.

Acknowledgments

We acknowledge the Colebrook Laboratory, a facility supported by the NIHR Imperial Biomedical Research Centre (BRC), for providing bioinformatics resources. Part of the bioinformatics analysis

was performed on equipment purchased as part of MRC CARP fellowship award MR/T005254/1. We also thank the Institut Pasteur teams for the curation and maintenance of BIGSdb-Pasteur databases at http://bigsdb.pasteur.fr.

Author contributions

Conceptualisation: KLH and YW; Resources: KLH, JT, GF, FM, NW, and GMR; Methodology: KLH, YW, JLCW, and EJ; Data curation: YW; Investigation and formal analysis: YW, JLCW, JSG, WWL, JT, FM, GMR, KD, IB, GF, EJ, DM, and KLH; Visualisation: YW; Writing – original draft: YW, JLCW, JSG, WWL, GMR, and KLH; Writing – review and editing: all authors.

Conflicts of interest

Authors declare that there are no conflicts of interest.

Consent to publish

No sensitive information is disclosed in this manuscript.

Ethical statement

National surveillance of communicable diseases and outbreak investigation work at UKHSA does not require individual patient consent as per Regulation 3 of The Health Service (Control of Patient Information) Regulations 2002.

References

1. **Baldwin CM, Lyseng-Williamson KA, Keam SJ**. Meropenem. *Drugs* 2008;68:803–838.
2. **Meini S, Tascini C, Cei M, Sozio E, Rossolini GM**. AmpC β-lactamase-producing Enterobacterales: what a clinician should know. *Infection* 2019;47:363–375.

3. **Livermore DM**. Defining an extended-spectrum β-lactamase. *Clinical Microbiology and Infection* 2008;14:3–10.

4. **Tooke CL, Hinchliffe P, Bragginton EC, Colenso CK, Hirvonen VHA, *et al.*** β-Lactamases and β-Lactamase Inhibitors in the 21st Century. *Journal of Molecular Biology* 2019;431:3472–3500.

5. **Jacoby GA**. AmpC β-Lactamases. *Clinical Microbiology Reviews* 2009;22:161–182.

6. **Jorgensen SCJ, Rybak MJ**. Meropenem and Vaborbactam: Stepping up the Battle against Carbapenem-resistant Enterobacteriaceae. *Pharmacotherapy: The Journal of Human Pharmacology and Drug Therapy* 2018;38:444–461.

7. **Rodloff AC, Goldstein EJC, Torres A**. Two decades of imipenem therapy. *Journal of Antimicrobial Chemotherapy* 2006;58:916–929.

8. **Prajapati JD, Kleinekathöfer U, Winterhalter M**. How to Enter a Bacterium: Bacterial Porins and the Permeation of Antibiotics. *Chem Rev* 2021;121:5158–5192.

9. **Lomovskaya O, Sun D, Rubio-Aparicio D, Nelson K, Tsivkovski R, *et al.*** Vaborbactam: Spectrum of Beta-Lactamase Inhibition and Impact of Resistance Mechanisms on Activity in Enterobacteriaceae. *Antimicrobial Agents and Chemotherapy* 2017;61:10.1128/aac.01443-17.

10. **Ehmann DE, Jahić H, Ross PL, Gu R-F, Hu J, *et al.*** Kinetics of Avibactam Inhibition against Class A, C, and D β-Lactamases. *Journal of Biological Chemistry* 2013;288:27960–27971.

11. **Carcione D, Siracusa C, Sulejmani A, Leoni V, Intra J**. Old and New Beta-Lactamase Inhibitors: Molecular Structure, Mechanism of Action, and Clinical Use. *Antibiotics* 2021;10:995.

12. **UK Health Security Agency**. UK Access, Watch, Reserve, and Other classification for antibiotics (UK-AWaRe antibiotic classification). https://www.gov.uk/government/publications/uk-aware-antibiotic-classification/uk-access-watch-reserve-and-other-classification-for-antibiotics-uk-aware-antibiotic-classification (2025).

13. **Sun D, Rubio-Aparicio D, Nelson K, Dudley MN, Lomovskaya O**. Meropenem-Vaborbactam Resistance Selection, Resistance Prevention, and Molecular Mechanisms in Mutants of KPC-Producing *Klebsiella pneumoniae*. *Antimicrobial Agents and Chemotherapy* 2017;61:e01694-17.

14. **Gaibani P, Bovo F, Bussini L, Lazzarotto T, Amadesi S, *et al.*** Dynamic evolution of imipenem/relebactam resistance in a KPC-producing *Klebsiella pneumoniae* from a single patient during ceftazidime/avibactam-based treatments. *Journal of Antimicrobial Chemotherapy* 2022;77:1570–1577.

15. **Gaibani P, Re MC, Campoli C, Viale PL, Ambretti S**. Bloodstream infection caused by KPC-producing *Klebsiella pneumoniae* resistant to ceftazidime/avibactam: epidemiology and genomic characterization. *Clinical Microbiology and Infection* 2020;26:516.e1-516.e4.

16. **Satapoomin Naphat, Dulyayangkul Punyawee, Avison Matthew B.** *Klebsiella pneumoniae* Mutants Resistant to Ceftazidime-Avibactam Plus Aztreonam, Imipenem-Relebactam, Meropenem-Vaborbactam, and Cefepime-Taniborbactam. *Antimicrobial Agents and Chemotherapy* 2022;66:e02179-21.

17. **Gaibani P, Giani T, Bovo F, Lombardo D, Amadesi S, *et al.*** Resistance to Ceftazidime/Avibactam, Meropenem/Vaborbactam and Imipenem/Relebactam in Gram-Negative MDR Bacilli: Molecular Mechanisms and Susceptibility Testing. *Antibiotics* 2022;11:628.

18. **Gaibani Paolo, Bianco Gabriele, Amadesi Stefano, Boattini Matteo, Ambretti Simone, *et al.*** Increased *bla*$_{KPC}$ Copy Number and OmpK35 and OmpK36 Porins Disruption Mediated Resistance to Imipenem/Relebactam and Meropenem/Vaborbactam in a KPC-Producing *Klebsiella pneumoniae* Clinical Isolate. *Antimicrobial Agents and Chemotherapy* 2022;66:e00191-22.

19. **Wilson WR, Kline EG, Jones CE, Morder KT, Mettus RT, *et al.*** Effects of KPC Variant and Porin Genotype on the In Vitro Activity of Meropenem-Vaborbactam against Carbapenem-Resistant Enterobacteriaceae. *Antimicrobial Agents and Chemotherapy* 2019;63:10.1128/aac.02048-18.

20. **Humphries Romney M., Hemarajata Peera**. Resistance to Ceftazidime-Avibactam in *Klebsiella pneumoniae* Due to Porin Mutations and the Increased Expression of KPC-3. *Antimicrobial Agents and Chemotherapy* 2017;61:10.1128/aac.00537-17.

21. **Turton JF, Payne Z, Coward A, Hopkins KL, Turton JA, *et al.*** Virulence genes in isolates of *Klebsiella pneumoniae* from the UK during 2016, including among carbapenemase gene-positive hypervirulent K1-ST23 and 'non-hypervirulent' types ST147, ST15 and ST383. *Journal of Medical Microbiology* 2018;67:118–128.

22. **The European Committee on Antimicrobial Susceptibility Testing**. Clinical breakpoints (v 15.0). https://www.eucast.org/fileadmin/src/media/PDFs/EUCAST_files/Breakpoint_tables/v_15.0_Breakpoint_Tables.xlsx (2025).

23. **Bolger AM, Lohse M, Usadel B**. Trimmomatic: a flexible trimmer for Illumina sequence data. *Bioinformatics* 2014;30:2114–2120.

24. **Chen S, Zhou Y, Chen Y, Gu J**. fastp: an ultra-fast all-in-one FASTQ preprocessor. *Bioinformatics* 2018;34:i884–i890.

25. **Wood DE, Lu J, Langmead B**. Improved metagenomic analysis with Kraken 2. *Genome Biology* 2019;20:257.

26. **Lu J, Breitwieser FP, Thielen P, Salzberg SL**. Bracken: Estimating species abundance in metagenomics data. *PeerJ Computer Science* 2017;2017:e104.

27. **Bouras G, Houtak G, Wick RR, Mallawaarachchi V, Roach MJ, *et al.*** Hybracter: Enabling Scalable, Automated, Complete and Accurate Bacterial Genome Assemblies. 2023;2023.12.12.571215.

28. **Bouras G, Sheppard AE, Mallawaarachchi V, Vreugde S**. Plassembler: an automated bacterial plasmid assembly tool. *Bioinformatics* 2023;39:btad409.

29. **Bouras G, Grigson SR, Papudeshi B, Mallawaarachchi V, Roach MJ**. Dnaapler: A tool to reorient circular microbial genomes. *Journal of Open Source Software* 2024;9:5968.

30. Medaka. github.com/nanoporetech/medaka.

31. **Bouras G**. pypolca. https://github.com/gbouras13/pypolca (2024, accessed 29 February 2024).

32. **Wick RR, Holt KE**. Polypolish: Short-read polishing of long-read bacterial genome assemblies. *PLOS Computational Biology* 2022;18:e1009802.

33. **Chklovski A, Parks DH, Woodcroft BJ, Tyson GW**. CheckM2: a rapid, scalable and accurate tool for assessing microbial genome quality using machine learning. *Nature Methods* 2023;20:1203–1212.

34. **Pedersen BS, Quinlan AR**. Mosdepth: quick coverage calculation for genomes and exomes. *Bioinformatics* 2018;34:867–868.

35. **Schwengers O, Jelonek L, Dieckmann MA, Beyvers S, Blom J, *et al.*** Bakta: rapid and standardized annotation of bacterial genomes via alignment-free sequence identification. *Microbial Genomics* 2021;7:000685.

36. **Lam MMC, Wick RR, Watts SC, Cerdeira LT, Wyres KL, *et al.*** A genomic surveillance framework and genotyping tool for *Klebsiella pneumoniae* and its related species complex. *Nature Communications* 2021;12:4188.

37. **Wyres KL, Wick RR, Gorrie C, Jenney A, Follador R, *et al.*** Identification of *Klebsiella* capsule synthesis loci from whole genome data. *Microbial Genomics* 2016;2:e000102.

38. **Feldgarden M, Brover V, Gonzalez-Escalona N, Frye JG, Haendiges J, *et al.*** AMRFinderPlus and the Reference Gene Catalog facilitate examination of the genomic links among antimicrobial resistance, stress response, and virulence. *Sci Rep* 2021;11:12728.

39. **Couvin D, Bernheim A, Toffano-Nioche C, Touchon M, Michalik J, *et al.*** CRISPRCasFinder, an update of CRISRFinder, includes a portable version, enhanced performance and integrates search for Cas proteins. *Nucleic Acids Research* 2018;46:W246–W251.

40. **Carattoli A, Zankari E, García-Fernández A, Voldby Larsen M, Lund O, *et al.*** *In Silico* Detection and Typing of Plasmids using PlasmidFinder and Plasmid Multilocus Sequence Typing. *Antimicrobial Agents and Chemotherapy* 2014;58:3895–3903.

41. **Robertson J, Nash JHE**. MOB-suite: software tools for clustering, reconstruction and typing of plasmids from draft assemblies. *Microbial Genomics*;4. Epub ahead of print 2018. DOI: https://doi.org/10.1099/mgen.0.000206.

42. **Ross Karen, Varani Alessandro M., Snesrud Erik, Huang Hongzhan, Alvarenga Danillo Oliveira, *et al.*** TnCentral: a Prokaryotic Transposable Element Database and Web Portal for Transposon Analysis. *mBio* 2021;12:10.1128/mbio.02060-21.

43. **Siguier P, Perochon J, Lestrade L, Mahillon J, Chandler M**. ISfinder: the reference centre for bacterial insertion sequences. *Nucleic Acids Research* 2006;34:D32–D36.

44. **Li H**. Minimap2: pairwise alignment for nucleotide sequences. *Bioinformatics* 2018;34:3094–3100.

45. **Cingolani P, Platts A, Wang LL, Coon M, Nguyen T, *et al.*** A program for annotating and predicting the effects of single nucleotide polymorphisms, SnpEff. *Fly* 2012;6:80–92.

46. **Jones P, Binns D, Chang H-Y, Fraser M, Li W, *et al.*** InterProScan 5: genome-scale protein function classification. *Bioinformatics* 2014;30:1236–1240.

47. **Ittisoponpisan S, Islam SA, Khanna T, Alhuzimi E, David A, *et al.*** Can Predicted Protein 3D Structures Provide Reliable Insights into whether Missense Variants Are Disease Associated? *Journal of Molecular Biology* 2019;431:2197–2212.

48. **The UniProt Consortium**. UniProt: a worldwide hub of protein knowledge. *Nucleic Acids Research* 2019;47:D506–D515.

49. **Zhou Y, Pan Q, Pires DEV, Rodrigues CHM, Ascher DB**. DDMut: predicting effects of mutations on protein stability using deep learning. *Nucleic Acids Research* 2023;51:W122–W128.

50. **Low WW, Wong JLC, Beltran LC, Seddon C, David S, *et al.*** Mating pair stabilization mediates bacterial conjugation species specificity. *Nature Microbiology* 2022;7:1016–1027.

51. **Alikhan N-F, Petty NK, Ben Zakour NL, Beatson SA**. BLAST Ring Image Generator (BRIG): simple prokaryote genome comparisons. *BMC Genomics* 2011;12:402.

52. **Grant JR, Enns E, Marinier E, Mandal A, Herman EK, *et al.*** Proksee: in-depth characterization and visualization of bacterial genomes. *Nucleic Acids Research* 2023;51:W484–W492.

53. **Wilkins D, Kurtz Z**. gggenes. wilkox.org/gggenes.

54. **Wong JLC, Romano M, Kerry LE, Kwong H-S, Low W-W, *et al.*** OmpK36-mediated Carbapenem resistance attenuates ST258 *Klebsiella pneumoniae in vivo*. *Nature Communications* 2019;10:3957.

55. **Teufel F, Almagro Armenteros JJ, Johansen AR, Gíslason MH, Pihl SI, *et al.*** SignalP 6.0 predicts all five types of signal peptides using protein language models. *Nat Biotechnol* 2022;40:1023–1025.

56. **The European Committee on Antimicrobial Susceptibility Testing**. MIC determination of non-fastidious and fastidious organisms. https://www.eucast.org/ast_of_bacteria/mic_determination.

57. **The European Committee on Antimicrobial Susceptibility Testing**. Guidance document on broth microdilution testing of cefiderocol. https://www.eucast.org/fileadmin/src/media/PDFs/EUCAST_files/Guidance_documents/Cefiderocol_MIC_testing_EUCAST_guidance_document_January_2024.pdf (2024).

58. **Ke W, Bethel CR, Thomson JM, Bonomo RA, van den Akker F**. Crystal Structure of KPC-2: Insights into Carbapenemase Activity in Class A β-Lactamases. *Biochemistry* 2007;46:5732–5740.

59. **Gato E, Guijarro-Sánchez P, Alonso-García I, Pedraza-Merino R, Conde A, *et al.*** *In vitro* development of imipenem/relebactam resistance in KPC-producing *Klebsiella pneumoniae* involves multiple mutations including OmpK36 disruption and KPC modification. *International Journal of Antimicrobial Agents* 2023;62:106935.

60. **Krishnan NP, Nguyen NQ, Papp-Wallace KM, Bonomo RA, van den Akker F**. Inhibition of *Klebsiella* β-Lactamases (SHV-1 and KPC-2) by Avibactam: A Structural Study. *PLOS ONE* 2015;10:e0136813.

61. **Pemberton Orville A., Tsivkovski Ruslan, Totrov Maxim, Lomovskaya Olga, Chen Yu**. Structural Basis and Binding Kinetics of Vaborbactam in Class A β-Lactamase Inhibition. *Antimicrobial Agents and Chemotherapy* 2020;64:10.1128/aac.00398-20.

62. **Holt KE, Wertheim H, Zadoks RN, Baker S, Whitehouse CA, *et al.*** Genomic analysis of diversity, population structure, virulence, and antimicrobial resistance in *Klebsiella pneumoniae*, an urgent threat to public health. *Proceedings of the National Academy of Sciences*. Epub ahead of print 2015. DOI: 10.1073/pnas.1501049112.

63. **Tsang KK, Lam MMC, Wick RR, Wyres KL, Bachman M, *et al.*** Diversity, functional classification and genotyping of SHV β-lactamases in *Klebsiella pneumoniae*. 2024;2024.04.05.587953.

64. **Huang Y, Lin Q, Zhou Q, Lv L, Wan M, *et al.*** Identification of *fosA10*, a Novel Plasmid-Mediated Fosfomycin Resistance Gene of *Klebsiella pneumoniae* Origin, in *Escherichia coli*. *IDR* 2020;13:1273–1279.

65. **Wan Y, Sabnis A, Mumin Z, Potterill I, Jauneikaite E, *et al.*** IS*1*-related large-scale deletion of chromosomal regions harbouring the oxygen-insensitive nitroreductase gene *nfsB* causes nitrofurantoin heteroresistance in *Escherichia coli*. *Microbial Genomics* 2023;9:001102.

66. **Sato T, Yamawaki K**. Cefiderocol: Discovery, Chemistry, and *In Vivo* Profiles of a Novel Siderophore Cephalosporin. *Clinical Infectious Diseases* 2019;69:S538–S543.

67. **Chen F-J, Lauderdale T-L, Ho M, Lo H-J**. The Roles of Mutations in *gyrA*, *parC*, and *ompK35* in Fluoroquinolone Resistance in *Klebsiella pneumoniae*. *Microbial Drug Resistance* 2003;9:265–271.

68. **Praski Alzrigat L, Huseby DL, Brandis G, Hughes D**. Fitness cost constrains the spectrum of marR mutations in ciprofloxacin-resistant *Escherichia coli*. *Journal of Antimicrobial Chemotherapy* 2017;72:3016–3024.

69. **Mori H, Ito K**. The Sec protein-translocation pathway. *Trends in Microbiology* 2001;9:494–500.

70. **Malinverni Juliana C., Silhavy Thomas J.** Assembly of Outer Membrane β-Barrel Proteins: the Bam Complex. *EcoSal Plus* 2011;4:10.1128/ecosalplus.4.3.8.

71. **Frankel G, David S, Low WW, Seddon C, Wong JLC, *et al.*** Plasmids pick a bacterial partner before committing to conjugation. *Nucleic Acids Res* 2023;51:8925–8933.

72. **Low Wen Wen, Seddon Chloe, Beis Konstantinos, Frankel Gad**. The Interaction of the F-Like Plasmid-Encoded TraN Isoforms with Their Cognate Outer Membrane Receptors. *Journal of Bacteriology* 2023;205:e00061-23.

73. **Rocker A, Lacey JA, Belousoff MJ, Wilksch JJ, Strugnell RA, *et al.*** Global Trends in Proteome Remodeling of the Outer Membrane Modulate Antimicrobial Permeability in *Klebsiella pneumoniae*. *mBio* 2020;11:10.1128/mbio.00603-20.

74. **National Institute for Health and Care Excellence**. Antimicrobial prescribing: meropenem with vaborbactam (Evidence summary [ES21]). *National Institute for Health and Care Excellence (NICE)*. https://www.nice.org.uk/advice/es21/chapter/Key-messages (2019).

620 75. **National Institute for Health and Care Excellence**. Ceftazidime with avibactam for treating
621 severe drug-resistant gram-negative bacterial infections (Health technology evaluation [HTE1]).
622 *National Institute for Health and Care Excellence (NICE)*.
623 https://www.nice.org.uk/guidance/hte1/chapter/1-Recommendations (2022).

624 76. **National Institute for Health and Care Excellence**. Antimicrobial prescribing: imipenem with
625 cilastatin and relebactam (Evidence summary [ES30]). *National Institute for Health and Care*
626 *Excellence (NICE)*. https://www.nice.org.uk/advice/es30/evidence (2020).

627 77. **Xu T, Guo Y, Ji Y, Wang B, Zhou K**. Epidemiology and Mechanisms of Ceftazidime–Avibactam
628 Resistance in Gram-Negative Bacteria. *Engineering* 2022;11:138–145.

629 78. **Sader HS, Mendes RE, Duncan L, Kimbrough JH, Carvalhaes CG, *et al.*** Ceftazidime-
630 avibactam, meropenem-vaborbactam, and imipenem-relebactam activities against multidrug-
631 resistant Enterobacterales from United States Medical Centers (2018–2022). *Diagnostic*
632 *Microbiology and Infectious Disease* 2023;106:115945.

633 79. **Hernández-García Marta, García-Castillo María, Bou Germán, Cercenado Emilia, Delgado-**
634 **Valverde Mercedes, *et al.*** Imipenem-Relebactam Susceptibility in Enterobacterales Isolates
635 Recovered from ICU Patients from Spain and Portugal (SUPERIOR and STEP Studies).
636 *Microbiology Spectrum* 2022;10:e02927-22.

637 80. **Shoulders BR, Casapao AM, Venugopalan V**. An Update on Existing and Emerging Data for
638 Meropenem-Vaborbactam. *Clinical Therapeutics* 2020;42:692–702.

639 81. **Guy RL, Hopkins KL, Budd EL, Wilson K, Fountain H, *et al.*** The importance of monitoring a
640 new antibiotic: ceftazidime/avibactam usage and resistance experience from England, 2016 to
641 2020. *Eurosurveillance* 2025;30:2400399.

642 82. **Sauerborn E, Corredor NC, Reska T, Perlas A, Vargas da Fonseca Atum S, *et al.*** Detection
643 of hidden antibiotic resistance through real-time genomics. *Nature Communications* 2024;15:5494.

644 83. **Theuretzbacher U, Carrara E, Conti M, Tacconelli E**. Role of new antibiotics for KPC-
645 producing *Klebsiella pneumoniae*. *Journal of Antimicrobial Chemotherapy* 2021;76:i47–i54.

646 84. **Sulavik MC, Gambino LF, Miller PF**. The MarR Repressor of the Multiple Antibiotic Resistance
647 (*mar*) Operon in *Escherichia coli*: Prototypic Member of a Family of Bacterial Regulatory Proteins
648 Involved in Sensing Phenolic Compounds. *Mol Med* 1995;1:436–446.

649 85. **Randall LP, Woodward MJ**. The multiple antibiotic resistance (*mar*) locus and its significance.
650 *Research in Veterinary Science* 2002;72:87–93.

651 86. **Martínez-Martínez L, Hernández-Allés S, Albertí S, Tomás J M, Benedi V J, *et al.*** *In vivo*
652 selection of porin-deficient mutants of *Klebsiella pneumoniae* with increased resistance to
653 cefoxitin and expanded-spectrum-cephalosporins. *Antimicrobial Agents and Chemotherapy*
654 1996;40:342–348.

655

Figures

Figure 1. Genetic structure of a 54.7-kbp region in KpMVS1 that was deleted in KpMVR1 (Table 4). Labels "start" and "end" indicate boundaries of the deleted region. Genes without known names are not labelled. Each asterisk indicates an allele from a named gene family.

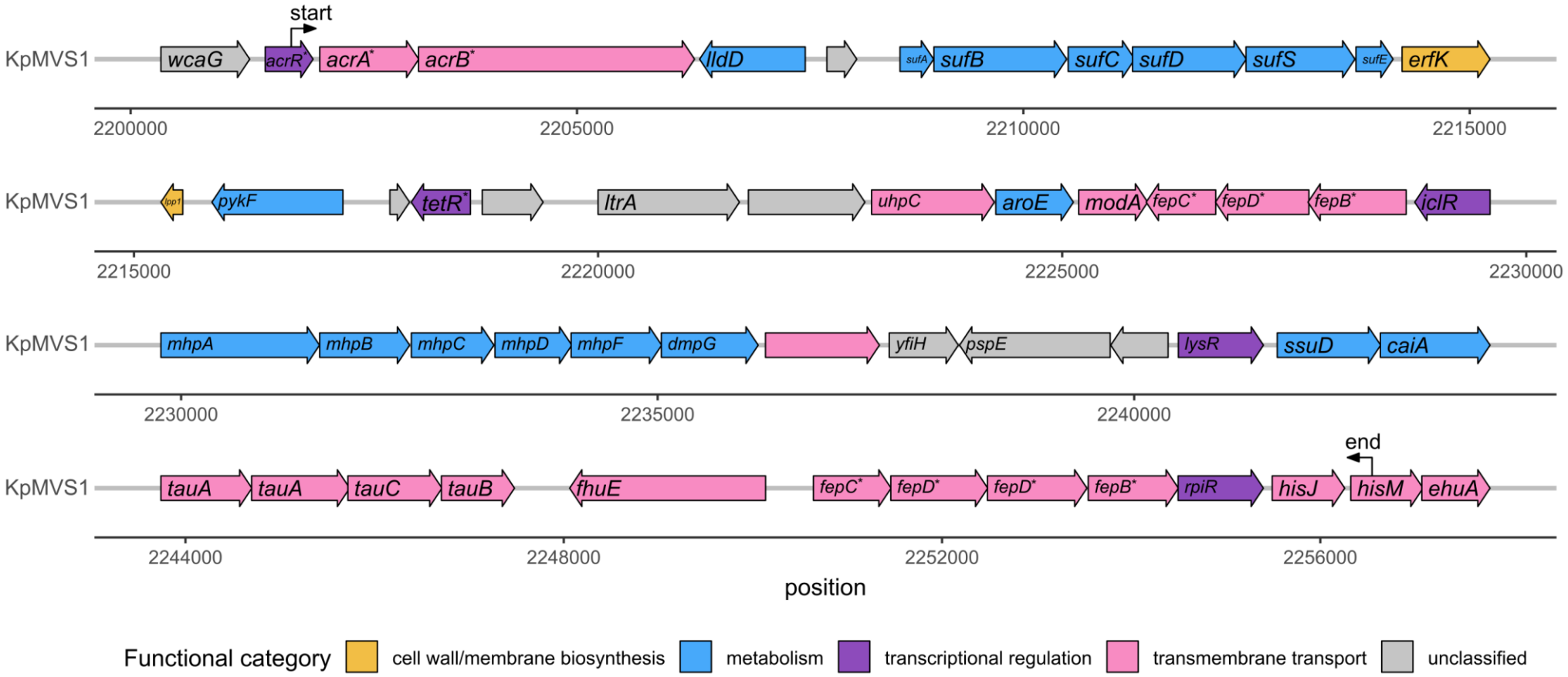

Figure 2. IS*Ec68*-mediated disruption of *ompK36* in isolate KpMVR1. (**A**) Genetic environment of the disrupted *ompK36* in KpMVR1. The arrow labelled "*ompK36**" denotes the upstream-shifted open reading frame caused by the insertion of IS*Ec68*. Abbreviations: CDS: coding sequence; IS, insertion sequence; ncRNA: non-coding RNA. (**B**) Comparison of predicted OmpK36 sequences using Clustal Omega (www.ebi.ac.uk/jdispatcher/msa/clustalo). Mismatches are highlighted in red, and the 22 N-terminal amino acids signal sequence of OmpK36 are indicated by the yellow shade. (**C**) Coomassie-stained polyacrylamide gel electrophoresis of outer membrane proteins to confirm the absence of OmpK36 in KpMVR1 and the *ompK36*-knockout isolate ICC8001$_{\Delta ompK36}$.